Development 126, 1149-1159 (1999)
Printed in Great Britain © The Company of Biologists Limited 1999
DEV4078

VEGF is required for growth and survival in neonatal mice

Hans-Peter Gerber, Kenneth J. Hillan, Anne M. Ryan, Joe Kowalski, Gilbert-Andre Keller, Linda Rangell, Barbara D. Wright, Freddy Radtke[1], Michel Aguet[1] and Napoleone Ferrara*

Departments of Cardiovascular Research and Pathology, Genentech, Inc., 1 DNA Way, South San Francisco, CA 94080, USA
[1]Present address: Swiss Institute for Experimental Cancer Research, 155 Chemin des Boveresses, 1066 Epalinges s/Lausanne, Switzerland
*Author for correspondence (E-mail: nf@gene.com)

Accepted 5 January; published on WWW 15 February 1999

SUMMARY

We employed two independent approaches to inactivate the angiogenic protein VEGF in newborn mice: inducible, Cre-*loxP*- mediated gene targeting, or administration of mFlt(1-3)-IgG, a soluble VEGF receptor chimeric protein. Partial inhibition of VEGF achieved by inducible gene targeting resulted in increased mortality, stunted body growth and impaired organ development, most notably of the liver. Administration of mFlt(1-3)-IgG, which achieves a higher degree of VEGF inhibition, resulted in nearly complete growth arrest and lethality. Ultrastructural analysis documented alterations in endothelial and other cell types. Histological and biochemical changes consistent with liver and renal failure were observed. Endothelial cells isolated from the liver of mFlt(1-3)-IgG-treated neonates demonstrated an increased apoptotic index, indicating that VEGF is required not only for proliferation but also for survival of endothelial cells. However, such treatment resulted in less significant alterations as the animal matured, and the dependence on VEGF was eventually lost some time after the fourth postnatal week. Administration of mFlt(1-3)-IgG to juvenile mice failed to induce apoptosis in liver endothelial cells. Thus, VEGF is essential for growth and survival in early postnatal life. However, in the fully developed animal, VEGF is likely to be involved primarily in active angiogenesis processes such as corpus luteum development.

Key words: Vascular endothelial growth factor (VEGF), VEGF receptors, Angiogenesis, Endothelium, Cre/*loxP*, Conditional gene targeting, Mouse, Body growth, Apoptosis

INTRODUCTION

The cardiovascular system is the first organ system to develop and reach a functional state in an embryo (Hamilton et al., 1962). The initial steps consist of 'vasculogenesis', the differentiation of endothelial cell precursors, the angioblasts, from the mesenchyme (Risau, 1995). The juvenile vascular system evolves from the primary capillary plexus by subsequent pruning and reorganization of endothelial cells in a process called 'angiogenesis'. This complex remodeling process involves the recruitment of mural cells and starts in almost all organ systems during late embryonic development (Nehls and Drenckhahn, 1993; Patan et al., 1997). Although vascularization occurs concomitantly to organ growth, surprisingly little is known about the role of endothelial cells and angiogenesis in regulating normal growth and organ homeostasis during postnatal development.

Several positive regulators of angiogenesis have been identified, including aFGF, bFGF, TGF-α, TGF-β, HGF, TNF-α, VEGF, angiogenin, IL-8 and the angiopoietins (for a review, see Carmeliet and Collen, 1998). Also, the αvβ3 integrin pathway has been shown to play a role in angiogenesis (Brooks et al., 1994). The negative regulators include thrombospondin (Good et al., 1990), the 16 kDa fragment of prolactin (Clapp et al., 1993), SPARC (Sage et al., 1995), angiostatin (O'Reilly et al., 1994) and endostatin (O'Reilly et al., 1997). The interplay between positive and negative regulators of angiogenesis is thought to give rise to the complex patterns of vascularization observed in different tissues and organs (Risau, 1997).

The endothelial cell-specific mitogen VEGF is a key mediator of normal and abnormal angiogenesis (Ferrara and Davis-Smyth, 1997). VEGF exerts its biological effects by binding to its respective tyrosine kinase receptors VEGFR1 (Flt-1) and VEGFR2 (Flk-1/KDR), both of which are expressed on endothelial cells. Mouse embryos null for either receptor die in utero between days 8.5 and 9.5 (Fong et al., 1995; Shalaby et al., 1995). Strong experimental evidence links Flk-1/KDR activation to VEGF-induced mitogenesis and angiogenesis (Ferrara and Davis-Smyth, 1997). In contrast, the function of Flt-1 is less clear and recent studies have unexpectedly shown that this receptor may perform its role in angiogenesis primarily as a ligand binding molecule, rather than as a signaling tyrosine kinase (Hiratsuka et al., 1998). VEGF is essential for embryonic development and loss of even a single VEGF allele results in embryonic lethality (Carmeliet et al., 1996; Ferrara et al., 1996).

Several lines of evidence suggest that VEGF is not only a mitogen but also a survival factor for newly formed blood vessels. However, this pro-survival role in vivo has only been

found so far for immature retinal vessels (Alon et al., 1995; Benjamin et al., 1998), or tumor-associated microvessels (Borgström et al., 1998; Yuan et al., 1996).

To address the role of VEGF in postnatal development, we sought to inactivate this factor by two independent approaches: Cre-*loxP*-mediated gene ablation after administration of interferon-α or of a soluble VEGF receptor chimeric protein, mFlt(1-3)-IgG. Our results demonstrate that VEGF is not only a critical regulator of organ and body size but, unexpectedly, that it is also essential for survival in early postnatal life.

MATERIALS AND METHODS

Construction of targeting vector and introduction in ES cells

A 18-kb genomic VEGF genomic clone encompassing exons 1 to 4 of the murine VEGF locus (Ferrara et al., 1996) was used to generate a 1.9 kb *Bam*HI-*Xba*I fragment encoding exon 2 of VEGF, which was blunt end cloned into the *Not*I site of TNLOX1-3 targeting vector. A 1.6 kb *Xba*I-*Eco*RI fragment, encoding exon 3, was blunt end cloned into the *Asc*I site and a 3.4 kb *Eco*RI-*Kpn*I fragment, including exon 4, was blunt end cloned into the *Pme*I site. All *loxP*-sites of the targeting vector TNBCE were sequenced and the orientation of the inserts verified by restriction digestion and sequencing. The targeting vector was linearized by *Sal*I digestion and 20 μg were used for electroporation of the ESGS clone derived from 129Sv ES cells. Characterization of this ES cell line and tissue culture conditions have been described previously (Huang et al., 1993). Briefly, cells were cultured on mouse embryonic fibroblast layer in the presence of 1000 i.u./ml of murine LIF (Gibco) in high glucose DMEM (Gibco) supplemented with 10% fetal bovine serum (FBS). Cells were subjected to G418 selection (400 μg/ml) and single colonies were analyzed for positive recombination events by Southern blot. The probe was generated by random prime labeling of a 1.8 kb *Bam*HI fragment derived from the 5′ upstream region of the VEGF locus. The genomic DNA was digested with *Kpn*I and *Sac*II and positive clones were identified by generation of a new 12 kb fragment in addition to the 10 kb wild-type allele. Positive recombination events were observed at a frequency of 1:100. Subsequently, colonies were analyzed for complete recombination of the 3′ region, including the *loxP*-3 site, by PCR analysis using oligonucleotides VEGFc5R.2 (ACA TCT GCT GTG CTG TAG GAA G) and VEGFe3.F (GAC CTG AAT TCG CGC CAT AAC T). Three independent ESGS clones were selected and transiently transfected with an expression vector encoding CRE recombinase (pMC-Cre) fused to the nuclear location signal of SV40 large T-antigen. 100 colonies were selected randomly and analyzed by PCR and Southern blot analysis for loss of the PGK-NEO gene and the flanking *loxP*-site. This was monitored by reduction of the PCR fragment from 2.5 kb to 0.9 kb applying the *loxP*-specific oligonucleotide VEGFb3lox.F (TCT AGG GCC GCC TCG AGA TAA C) and VEGFex.R (CAT CGT TAC AGC AGC CTG CAC A). The latter oligonucleotide was designed to hybridize to exon 3 of the mouse VEGF gene. The presence of the *loxP*-3 sequence was verified using oligonucleotides VEGFc5R.2 and VEGFe3.F. Selected ES colonies were grown to confluency and VEGF levels in the supernatant were determined by a radioreceptor assay using Flk-1/KDR-IgG (Presta et al., 1997). The genomic DNA isolated from these clones was digested with *Eco*RI and analyzed by Southern blotting using the random primed 1.8 kb *Bam*HI 5′ probe described above.

Generation of VEGF/loxP mice

One derivative of each ES cell line containing the floxed VEGF allele was injected into the blastocoele cavity of 3.5-day C57BL/6J blastocysts (Hogan et al., 1994). Chimeric males were mated with C57BL/6J females and agouti offsprings were screened for germline transmission by PCR analysis for VEGF alleles containing the *loxP*-1 and *loxP*-3 sites. Heterozygous VEGF– *loxP*– males were bred to MX-1-Cre mice to generate VEGF–*loxP*–(+/–), MX-1-Cre(+) mice and these were bred by brother-sister mating to VEGF- *loxP*–(+/+), MX-1-Cre(+) mice. Mice were bred to homozygosity based on PCR analysis of tail DNA using primer pairs muVEGF419.F (CCT GGC CCT CAA GTA CAC CTT) and muVEGF567.R (TCC GTA CGA CGC ATT TCT AG), which generate a 148 bp fragment of the VEGF allele in the presence of the *loxP*-1 site, and a shorter fragment of about 40 bp for the wild-type allele. The presence of the MX-1 Cre transgene was verified by tail DNA PCR using the oligonucleotides CRE1 (CCT GTT ACG TAT AGC CGA AAT) and CRE2 (CTA CAC CAG AGA CGG AAA TC).

VEGF gene ablation by IFN-α administration

10000 units of recombinant murine IFN-α (Chemicon) were administered intraperitoneally to newborn mice at days 3, 5 and 7. 12-15 days after beginning of treatment, mice were killed and tissues were fixed for histological analyses or frozen in liquid nitrogen for determination of genotype and knock out efficiency in various tissues. DNA was prepared using the genomic DNA isolation kit from Qiagen. Knock out efficiency was assessed by ‘real time’ quantitative PCR (TAQMAN) (Gibson et al., 1996; Heid et al., 1996) of genomic DNA isolated using probe/primer sets recognizing the ‘floxed’ VEGF alleles at the *loxP*-1 or the *loxP*-3 site. For determination of recombination efficiency at the *loxP*-3 site, VEGFc5Probe2 and primers VEGFc5R.2 and VEGFe3.F were used, and at the *loxP*-1 site, mVEGF 359.FP 5′(FAM)-TGG CAG GCT GAG CCA CCA TTT G-(TAMRA)p3′ and primers mVEGF322.F (ACT TCA TGG ACA GGC TTC GG) and mVEGF*loxP*-1.552.R (CTA GCG CGC CAT AAC TTC G) for *loxP*-1.

Treatment of mice with mFlt(1-3)-IgG

C57BL-6 newborn mice were injected intraperitoneally once daily starting at day 1 or day 8 post delivery with 25 mg/kg/day of mFlt(1-3)-IgG in PBS in a total volume of 50 μl per dose. mFlt(1-3)-IgG is a fusion protein consisting of the first three Ig-like domains of mFlt-1 fused to a murine Fc (γ2B) (Ferrara et al., 1998). Previous studies have shown that this truncated soluble receptor has the same binding characteristics as Flt(1-7)-IgG, but its half-life following systemic administration is substantially longer (Davis-Smyth et al., 1996). mFlt(1-3)-IgG was purified and characterized as previously described (Ferrara et al., 1998). Controls were a murine anti-gp120 monoclonal antibody of same IgG isotype as the Fc in mFlt(1-3)-IgG, administered at the same dose, or PBS. Body mass measurements were taken daily. After treatment, animals were killed by pentobarbital administration and the tissues were harvested and fixed.

Capillary counts

All tissues for immunohistochemistry were formalin-fixed and paraffin-embedded. For capillary counts, immunohistochemistry was performed on kidney, liver, heart and lung sections from animals treated with control IgG or mFlt(1-3)-IgG. After a 20 minute exposure to AR10 (Biogenex) at 96°C, sections were incubated with a rat anti-murine Flk-1 monoclonal antibody at 3.9 μg/ml overnight at 4°C. This antibody (MALK-1), raised against recombinant mouse Flk-1(1-7)-IgG fusion protein, belongs to the IgG2A isotype. MALK-1 stains primarily non-arterial vascular endothelium. In contrast, an anti-CD31 antibody (Pharmingen) labels all vascular endothelial cells. Although changes in blood vessel density appeared qualitatively similar using both antibodies, MALK-1 gave a lower background and more consistent staining than anti-CD31. Therefore, data obtained with MALK-1 will be shown. A biotinylated rabbit antibody to rat IgG (Vector) was used as the secondary reagent and detected by the DuPont Tyramide Signal Amplification Kit (NEN Life Science Products). Purified rat IgG2A was used as a negative control. To quantitate blood vessel density, Flk-1-immunostained sections were examined through a 10×10 eyepiece grid under a 40× objective. At this magnification, the grid covered an area of 0.063 mm^2 (25 μm ×

25 μm). Random regions were selected such that the grid was filled with the parenchyma of each tissue. Each square within the grid that did not contain a Flk-1-positive endothelial cell was scored. The minimum possible score is 0 and the maximum score 500, where 500 would indicate a complete absence of Flk-1-positive cells. Five independent, randomly selected fields were counted from each organ of three animals. Data are shown as means ± s.d.

Cell proliferation analysis

Immunohistochemistry was performed on sections of BrdU-incorporated kidney, heart, liver and lung from control IgG or mFlt(1-3)-IgG-treated animals. BrdU was administered intraperitoneally to animals at a dose of 100 mg/kg, 1 hour prior to killing. After a 20-minute treatment with 0.05% trypsin at 37°C and a 45-minute treatment with 95% formamide in 0.15 M trisodium citrate at 70°C for denaturing, tissues were stained with mouse anti-IdU/BrdU (Caltag) at a dilution of 1:1000 overnight at 4°C. A biotinylated horse anti-mouse IgG (Vector) was used as the secondary reagent and detected by using the Vectastain ABC Standard Elite kit (Vector Laboratories). Mouse Isotype (Zymed) was used as a negative control. Sections were counterstained with Hematoxylin and labeled nuclei in ten independent, randomly selected, fields using a 40× objective were counted. Each field covered an area of 0.063 mm^2.

Electron microscopy

Tissues from control IgG and mFlt(1-3)-IgG treated animals were fixed for 2 hours in 2% formaldehyde, 2.5% glutaraldehyde in 0.1 M cacodylate buffer. After washing, the samples were postfixed in aqueous 1% osmium for 2 hours, washed in water, dehydrated through graded ethanols and propylene oxide, and embedded in EPONATE 12 (Ted Pella, Inc. Redding, Ca). Ultrathin sections were cut on a Reichert Ultracut E microtome, counterstained with uranyl acetate and lead citrate, examined in a Philips CM12 transmission electron microscope at 80 kV and images were captured with a GATAN Retractable Multiscan digital camera.

Isolation of liver endothelial cells and apoptosis analysis

Mice that had been treated for 3 days with mFlt(1-3)-IgG or control IgG were perfused with 10 ml of 1 mg/ml collagenase, 10 mg/ml, 10% FBS in Opti-MEM (Gibco) for 5 minutes. Livers were harvested and transferred to 10 ml of collagenase digestion buffer (Opti-MEM complemented with BSA (10 mg/ml, Bayer), 10% FBS (Gibco) and collagenase H (1 mg/ml). After mechanically dispersing the tissues into 1 mm^3 cubes, fragments were digested at 37°C for 30 minutes in 10 ml of collagenase digestion buffer. The resulting suspension was filtered through a Falcon 2350 restrainer cap (70 μm cut-off membrane). Cells were centrifuged for 5 minutes at 1000 rpm, and resuspended in Opti-MEM complemented with BSA (10 mg/ml) and 10% FBS. This washing procedure was repeated twice. Cells were resuspended in 1 ml of binding buffer (Opti-MEM, 10 mg/ml BSA, 10% FBS, 0.05% sodium azide) and incubated on ice with IgG2A rat anti mouse CD31-FITC (MEK 13.3, Pharmingen) at 5 μg/ml for about 30 minutes. Alternatively, cells were incubated with a biotin-conjugated anti-mouse Panendothelial Cell Antigen (5 μg/ml, MECA 32, Pharmingen) and 10 μl of FITC-conjugated avidin (Pharmingen). Cells were washed twice in Ca-binding buffer (10 mM Hepes/NaOH, pH 7.4, 140 mM NaCl, 2.5 mM $CaCl_2$). For apoptosis analysis, cells were immediately afterwards incubated with 10 μl of annexin-V-PE (R&D systems) in a total volume of 1 ml Ca-binding buffer for 15 minutes on ice prior to FACS analysis. The control PE-labeled antibody was IgG2A-PE (Becton Dickinson). Cells negative for both propidium iodide (PI) staining and annexin V binding, but CD31-positive, were considered to be live endothelial cells. PI-negative, annexin V- and CD31-positive cells were considered early apoptotic endothelial cells; PI-positive, annexin V- and CD31-positive cells are primarily cells in late stage of apoptosis (Moore et al., 1998).

RESULTS

Impaired growth following conditional VEGF gene inactivation

To elucidate the significance of VEGF in postnatal development, we applied the Cre-*loxP*-based conditional gene knock-out technology (Gu et al., 1994). A targeting vector was generated in which exon 3 of the mouse VEGF gene is flanked by *loxP* sites (Fig. 1A). We obtained VEGF*loxP*(+/–) and VEGF*loxP*(+/+) mice at the expected Mendelian ratio (data not shown). Analysis of VEGF release by ES cells revealed that

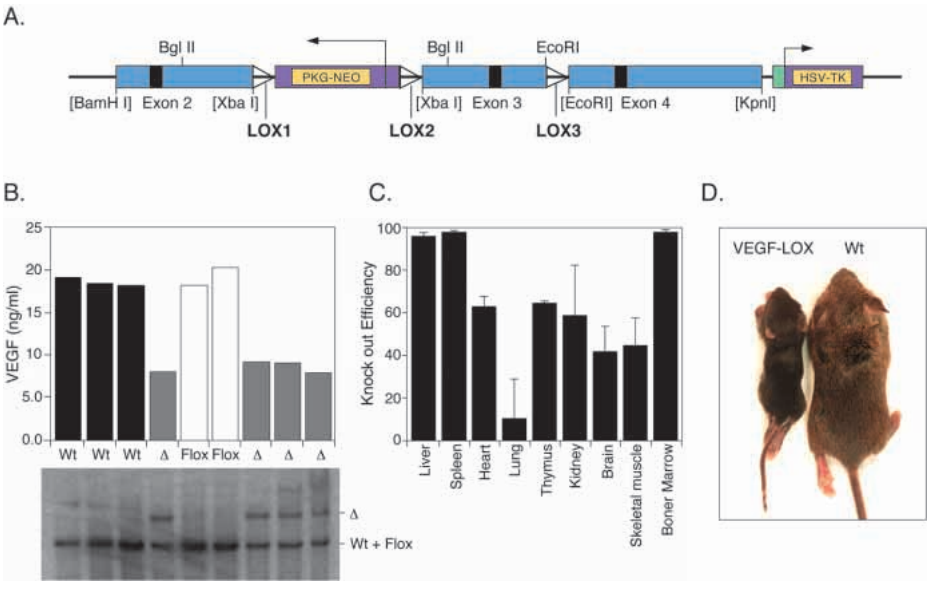

Fig. 1. Generation of conditional VEGF knock out mice. (A) Structure of the targeting vector. *loxP* sites were placed at the *Xba*I and *Eco*RI sites, respectively, flanking exon 3. (B) Southern blot analysis of ES cell clones containing both wild-type VEGF alleles (Wt), one wild-type and one floxed allele (Flox) or one wild-type and one allele deleted in exon 3 of VEGF (Δ), following transient transfection with Cre recombinase (pMC-Cre). The upper part of B indicates the levels of VEGF in the supernatant of each ES cell colony. (C) Knock out efficiencies in various organs after administration of 10,000 i.u. of IFN-α intraperitoneally at days 3, 5 and 7 postnatally. Data were generated by real-time PCR analysis using a LOX-3-specific probe primer set as described. The IL-8 receptor gene was used as reference. DNA of three 14-day-old VEGF*loxP*(+/+)Cre+ and three VEGF*loxP*(+/+)Cre– animals, which survived the treatment, were analyzed; values are ±s.d. (D) Comparison of body sizes between two 14-day-old littermates treated with 10,000 i.u. of IFN-α at days 3, 5 and 7. The VEGF*loxP*(+/+)Cre+ littermate is shown to the left while the VEGF*loxP*(–/–)Cre+ (wt) mouse is on the right.

Table 1. Analysis of growth retardation and mortality of newborn mice of different genotype

Genotype	% Mortality at day 7	% Growth retarded survivors*	% Animals with normal body mass at day 27
VEGF *loxP*(+/+) Cre+ (*n*=21)	38	52	10
VEGF *loxP*(+/–) Cre+ (*n*=6)	0	33	66
VEGF *loxP*(+/+) Cre– (*n*=10)	0	0	100

All groups were treated with 10,000 i.u. of IFN-α at days 3, 5 and 7 postnatally.
*Values >20% compared to control littermates were counted.

VEGF*loxP*(+/–) clones secrete similar levels of VEGF to wild-type ES cells, unless exon 3 has been deleted (Fig. 1B), suggesting that the two *loxP* sites do not interfere with normal VEGF expression. Mice containing the 'floxed' VEGF allele were bred to a strain transgenic for Cre recombinase controlled by an interferon (IFN)-α-responsive promoter (MX-1-Cre) (Kuhn et al., 1995). Intraperitoneal administration of recombinant mouse IFN-α to VEGF-*loxP*(+/+)Cre+ neonate mice resulted in knock out efficiencies in various organs ranging from 50% in the kidney to 95% in the liver, spleen and bone marrow (Fig. 1C). The lowest efficiency was detected in the lung (<30%). These findings probably reflect differences in the expression of IFN receptors as well as in the bioavailability of IFN-α in various tissues and organs (Kuhn et al., 1995). As indicated in Table 1, administration of IFN-α resulted in reduced body mass gain in VEGF*loxP*(+/+)Cre+ animals, while their VEGF*loxP*(+/+)Cre– littermates grew at normal rates (Table 1). Furthermore, 38% of VEGF *loxP*(+/+)Cre+ animals treated died around day 7. Interestingly, a trend toward reduced body growth was also observed in VEGF*loxP*(+/–)Cre+ mice following IFN-α administration, suggesting a dosage effect. However, IFN-α administration to 6- to 10-week-old VEGF*loxP*(+/+)Cre+ mice did not induce any significant changes in body or organ mass relative to age-matched VEGF*loxP*(+/+)Cre– mice.

Abnormal liver development in VEGF knockout mice

Consistent histological changes were observed in livers of 14-day-old VEGF*loxP*(+/+)Cre+ mice, treated with IFN-α (Fig. 2A,B). Hepatocytes were small and rounded and the hepatic sinusoidal architecture remained immature, with persistence of twin cell hepatic plates. In addition, many sinusoids contained prominent eosinophilic histiocytes. There was increased extramedullary hematopoiesis and almost complete absence of Flk-1-positive endothelial cells (Fig. 3C,D). The heart, kidney, lung and spleen were all within normal histological limits, albeit small in size. The more profound liver phenotype is consistent with the high knock out efficiency in this organ.

Inhibition of organ development and lethality in neonatal mice treated with mFlt(1-3)-IgG

To verify these findings by an independent approach, we used a truncated soluble Flt-1 receptor, mFlt(1-3)-IgG (Ferrara et al., 1998). Systemic administration of mFlt(1-3)-IgG resulted in almost complete inhibition of VEGF-induced angiogenesis in a rat model of hormonally induced ovulation (Ferrara et al., 1998). Initiation of treatment in neonatal mice either at day 1 or 8 postnatally resulted in reduced mass gain (Fig. 4A,C), more pronounced than that observed with Cre/*loxP*– mediated gene targeting. As little as 1 mg/kg of mFlt(1-3)-IgG administered daily resulted in a detectable inhibition compared

Table 2. Blood chemistry and hematology parameters following mFlt (1-3)-IgG or control IgG administration

Time after treatment	Glu (mg/dl)	BUN (mg/dl)	Alb (g/dl)	Total protein (g/dl)	K^+ (meq/l)
(A) Day 5					
Control IgG (*n*=14)	68±4	31±1	0.52±0.06	2.43±0.05	7.4±0.6
Flt (1-3)-IgG (*n*=11)	32±8*	45±6*	0.53±0.09	2.52±0.15	8.0±0.5
Day 14					
Control IgG (*n*=10)	89.7±3.5	25±1	1.3±0.2	3.1±0.1	8.6±0.6
Flt (1-3)-IgG (*n*=9)	57.1±9.3*	204±18*	0.7±0.3*	2.2±0.3*	13.1±1.2
	WBC (10^3/μl)	RBC (10^6/μl)	HGB (g/dl)	HCT (%)	PLT (10^3/μl)
(B) Day 5					
Control IgG (*n*=6)	7.9±1.1	3.4±0.1	10.2±0.3	27.4±0.9	521±13
Flt (1-3)-IgG (*n*=8)	12.3±1.0*	4.5±0.1	13.1±0.5	33.9±1.2	349± 46**
Day 14					
Control IgG (*n*=15)	4.6±0.4	5.3±0.1	9.9± 0.2	27.6±0.3	906±35
Flt (1-3)-IgG (*n*=9)	20.3±3.3*	5.3±0.3	11.7±0.6*	32.3±1.6*	520±50**

.
(A) Glucose (Glu), blood urea nitrogen (BUN), albumin (Alb) total protein (Pr) and potassium (K^+)) levels in the serum of animal treated with control IgG or mFlt(1-3)-IgG. Blood was collected at the time of killing.
In the day-5 groups, the treatment was initiated at day 1 and daily injections were given for 4 days.
In the day-14 groups, the treatment was initiated at day 8 and continued by daily injections.
The dose of both IgGs was 25 mg/kg daily. Values are means ± s.e.m. Values are significantly different, *P<0.05; **P<0.005.
(B) Hematological parameters of the above described groups. WBC, white blood cells; RBC, red blood cells; HGB, hemoglobin; HCT, hematocrit; PLT, platelets.

Table 3. Blood vessel absence determination in liver, heart and kidney and measurement of cell proliferation by BrdU labeling in liver, heart, lung and kidney of animals treated with control IgG or mFlt (1-3)-IgG

	Blood vessel quantification by Flk-1-positive cells		
	Liver	Heart	Kidney
Day 5			
Control IgG	7.3±2.5	2.7±2.1	124.3±11.6
Flt (1-3)-IgG	83.3±15.6	61.7±12.7	175.3±12.3
Day 14			
Control IgG	3.3±1.5	4.7±1.5	NA
Flt (1-3)-IgG	231.5±77.1	94.5±29.0	NA

	Cell proliferation (BrdU labeling)			
	Liver	Heart	Lung	Kidney
Day 5				
Control IgG	580.6±58	349.3±52.1	160.3±32.7	295.6±52.7
Flt (1-3)-IgG	298±74.1	37±20.5	13.0±2.7	105±33.7

The minimum possible score for the absence of blood vessels is 0, and the maximum score 500, where 500 would indicate a complete absence of Flk-1 positive cells.

In the day-5 groups, the treatment was initiated at day 1 and daily injections were given for 4 days.

In the day-14 groups, the treatment was initiated at day 8 and continued by daily injections.

to PBS- or mIgG-treated animals (data not shown). A maximum inhibitory effect was observed at the dose of 25 mg/kg daily. All animals treated with such a dose died within 4-6 days. The difference in mass gain and survival between mFlt(1-3)-IgG treated and Cre/*loxP*-animals may be explained by the partial VEGF inhibition achieved by the inducible targeting system, in contrast to the nearly complete inhibition with mFlt(1-3)-IgG (Ferrara et al., 1998). In view of the more profound phenotype obtained, most analyses were performed on mFlt(1-3)-IgG-treated animals.

At necropsy, all animals given mFlt(1-3)-IgG starting at day 1 or 8, were smaller than controls (Fig. 4A,B) and all major organs were reduced in size (Fig. 4C,D). However, similar amounts of milk were found in the stomach of control and mFlt(1-3)-IgG-treated groups, indicating that inadequate feeding is unlikely to be the cause of impaired growth. The most dramatic change in gross organ size were observed in the kidney (Fig. 4E), heart (Fig. 4F) and liver. The kidneys were shrunken, had a granular surface and showed focal interstitial hemorrhage.

Histopathogical analysis (Ribelin and Cox, 1965) revealed differences between the day-5 and day-14 groups. In day-5 animals, there was a striking reduction in brown fat stores, and some had thymic involution, suggesting severe metabolic stress. Some large vessels had focal adherence of leukocytes to the endothelium, and in some there was leukocytoclastic vasculitis (Fig. 2D), indicating vascular injury. No evidence of vasculitis was found in animals treated with control IgG. The kidneys showed interstitial hemorrhage at the corticomedullary junction (Fig. 4E). Juxtamedullary and cortical glomeruli were enlarged, hypocellular and showed accumulation of eosinophillic mesangial matrix. Glomerular capillary loop numbers were reduced compared to controls and proximal tubular epithelium contained protein droplets (data not shown). Ultrastuctural analysis of kidneys of treated animals showed that glomerular capillaries were underdeveloped and in some instances entirely missing. Interestingly, these alterations appeared to be mostly restricted to juxtamedullary glomeruli. There was an increased mesangial matrix (Fig. 5B,D) with granular material and proteinaceous deposits that included fibrin but no immune complexes were detected. The cytoplasmic foot processes of podocytes were normal in appearance and interacted with a thickened basement membrane. Interestingly, the capillaries in the peritubular regions showed normal fenestration in about half the profiles surveyed (Fig. 5F). Kidneys from animals given control IgG appeared normal (Fig. 5A,C,E).

In the liver, portal tracts were small and hypercellular and the sinusoidal architecture showed persistence of the fetal vascular pattern (Ribelin and Cox, 1965). Ultrastructural analysis showed that livers of the treated animals had reduced numbers of endothelial cells and focal loss of integrity of the space of Disse (Fig. 6B). When the endothelial cells were absent, hematopoietic cells could be often seen in direct contact with the hepatocyte plasma membrane. Bile canaliculi displayed normal morphology. The controls showed normal morphology (Fig. 6A).

In the heart, single cell necrosis of cardiomyocytes was observed (Fig. 2C) and the lungs from treated animals appeared immature, with less complex alveolar patterning (Fig. 2G,H). Spotty single cell necrosis was also observed in the liver, pancreas and spinal ganglia (data not shown).

In the day-14 group, a striking glomerulopathy, affecting all glomeruli, was observed (Fig. 2E,F). Glomeruli were uniformly enlarged and hypocellular, and mesangial cells showed cytoplasmic vacuolation. In the liver of mFlt(1-3)-IgG-treated animals, microvesicular steatosis was present and occasional apoptotic cells were observed within the hepatic parenchyma. In Fig. 6, the depletion cells lining the sinusoids in the treated group is evident. At this stage, heart, lung, intestine and pancreas all appeared histologically normal. Interestingly, in contrast to the day-5 treatment group, there was only a modest decrease in the adipose tissue content in the day-14 group following mFlt(1-3)-IgG treatment.

Table 4. Apoptosis in endothelial cells after treatment with mFlt (1-3)-IgG or control IgG

	CD31 positive	Apoptotic, CD31 positive
Day 11		
Control IgG (*n*=3)	18.9±1.9	2.1±0.4
Flt(1-3)-IgG (*n*=3)	4.1±0.3*	14.3±2.1*
Day 27		
Control IgG (*n*=4)	16.3±3.1	4.0±0.4
Flt(1-3)-IgG (*n*=4)	15.2±2.1	4.0±1.2

In the day-11 group, animals were treated for 3 days with control IgG or mFlt (1-3)-IgG, starting at day 8 postnatally.

In the day-27 group, the same treatment was initiated at day 24.

The dose of both IgGs was 25 mg/kg daily.

Isolation of endothelial cells and apoptosis assessment by FACS were performed as described in Materials and methods.

Values are % of total and are means±s.e.m. *Significantly different $P<0.005$.

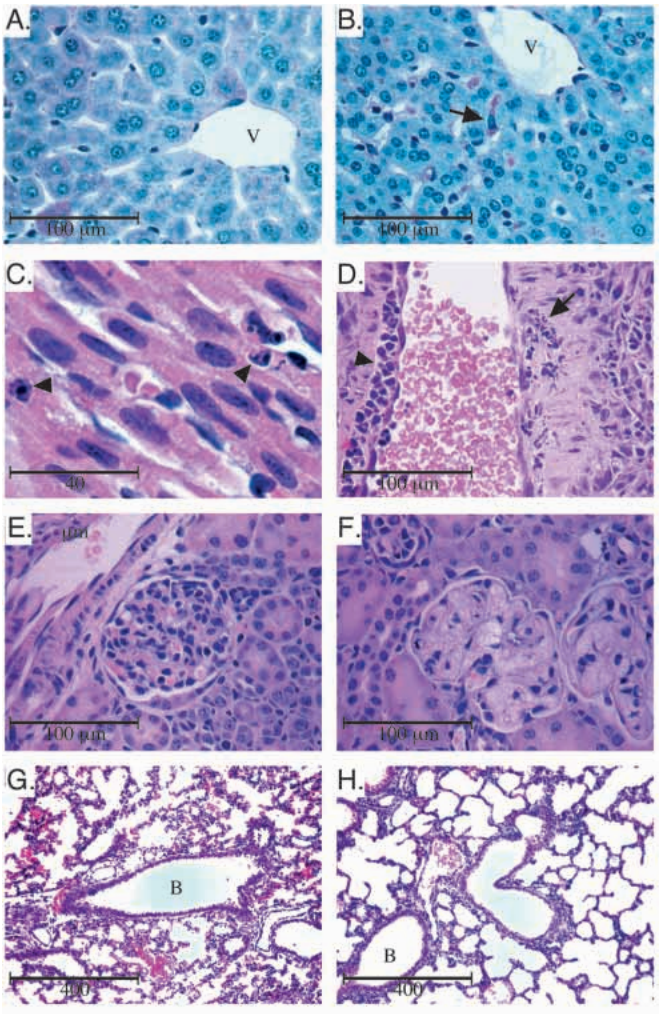

Fig. 2. PAS stained images from the perivenular (V) region of the liver from control (A) and VEGF*loxP*(+/+)Cre+ mice treated with IFN-α (B). The hepatocytes in VEGF knock out animals were smaller, more densely packed and the sinusoidal architecture had failed to mature into the normal adult pattern of single cell hepatocyte plates. Frequent PAS-positive cells were seen within hepatic sinusoids, and the cells have the morphological features of macrophages (arrow) of KO mice. (C) Hematoxylin and eosin staining of the heart of a 5-day-old neonate treated with mFlt(1-3)-IgG, showing apoptotic myocytes (arrowhead), and of the lumen and wall of a vein of a 5-day-old neonate treated with mFlt(1-3)-IgG (D), showing adherence of leukocytes to endothelium, sub-endothelial leukocyte infiltration (arrowhead) and areas of necrosis in the vascular wall (arrow). (E,F) Hematoxylin and eosin staining of glomeruli from 14-day-old animals treated for 5 days with control antibody (E) or mFlt(1-3)-IgG (F). The enlarged, hypocellular glomeruli contained few capillary loops and were filled with large vacuolated cells. (G,H) Hematoxylin and eosin staining of lungs from 5-day-old control (G) or treated (H) animals The lungs from mFlt(1-3)-IgG-treated animals appeared immature, with less complex alveolar patterning. B, main bronchus. Bars, 40 μm (C,D); 100 μm (A,B,E,F); 400 μm (G,H).

Administration of mFlt(1-3)-IgG to adult mice for 2 or 4 weeks failed to induce any significant changes in body mass relative to controls. All the major organs were normal by histological examination (data not shown).

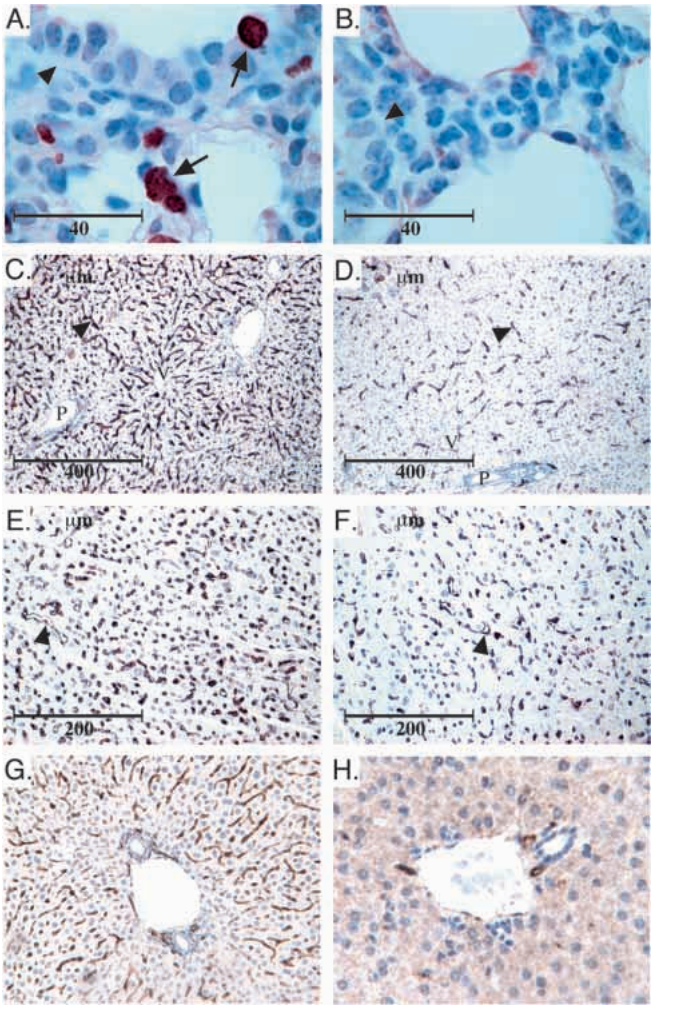

Fig. 3. BrdU labeling of lung and Flk-1 immunostaining of liver and heart. (A,B) BrdU labeling of sections of lung of 5-day-old control IgG (A) or mFlt(1-3)-IgG-treated mice (B). More positively labeled cells (arrows) were seen in control animals (arrowhead points to bronchial epithelium). (C,D) Flk-1 immunostaining of livers from control (C) and mFlt(1-3)-IgG-treated mice (D). Arrowheads point towards Flk-1 staining in sinusoidal endothelium. Arrows point toward Flk-1 staining on venular endothelium in a portal tract. P, portal tract; V, terminal hepatic venule. Bars, 400 μm. (E,F) Flk-1 immunostaining of hearts from 5-day-old mice treated with control antibody (E) or mFlt(1-3)-IgG (F). Positively labeled vessels are marked (arrowhead). (G,H) Flk-1 immunostaining of livers of 14-day-old VEGF*loxP*(+/+)Cre– (G) and VEGF*loxP*(+/+)Cre+ (H) mice, both treated with IFN-α as described in the text. Bars, 40 μm (A,B); 200 μm (E,F); 400 μm (C,D).

Severe renal failure and tissue hypoxemia in mFlt(1-3)-IgG-treated neonates

In agreement with the histopathological picture of kidney and liver damage, the levels for blood urea nitrate (BUN) were increased, especially in the group where mFlt(1-3)-IgG treatment was initiated at day 8 (Table 2). Decreased levels of albumin and total proteins are also consistent with this picture (West, 1990). Also, consistent with kidney failure, mFlt(1-3)-IgG-treated animals in the day 8-group demonstrated critically elevated serum K^+ levels (Table 2), a

change expected to predispose to cardiac arrhythmias (West, 1990).

Increases in hematocrit and hemoglobin levels were observed in animals at both age groups following mFlt(1-3)-IgG treatment (Table 2). Quantitative PCR analysis (Gibson et al., 1996) demonstrated a 3- to 6-fold increase in erythropoietin expression in the kidney (data not shown). These findings are consistent with a homeostatic response to systemic hypoxemia (Jelkmann, 1992) resulting from pulmonary and cardiac hypoplasia. Interestingly, animals treated with mFlt(1-3)-IgG in both age groups had significantly lower platelet counts than controls (Table 2).

Reduced proliferation rates and increased apoptotic index among parenchymal cells correlate with a reduction in capillary vessels

Immunohistochemistry for the endothelial cell markers CD31 (data not shown) and Flk-1 revealed a reduction in the number and complexity of capillary vessels in the kidneys, livers and hearts of mFlt(1-3)-IgG-treated animals (Fig. 3E-H; Table 3). To quantify cell proliferation in the day-5 animals, BrdU labeling was performed. Proliferation was reduced in the liver, heart, lung and kidneys of treated animals (Fig. 3A,B; Table 3).

In situ hybridization showed that VEGF and Flk-1 mRNAs were widely expressed, in agreement with previous studies (Monacci et al., 1993; Quinn et al., 1993). Flk-1 showed expression on endothelial cells in a distribution which, for the most part, complemented that observed with VEGF. The major change observed in mFlt(1-3)-IgG animals was a reduction in Flk-1 mRNA expression in the lung, similar to that observed by immunohistochemistry (data not shown). To determine whether apoptosis contributed to the observed impairment in body growth, we performed apoptag labeling. Increased apoptosis was significant in lymphoid cells of the thymus and hearts of day-5 group (Fig. 2C).

Age-dependent endothelial cell apoptosis following VEGF inhibition

To determine directly whether decreased levels of VEGF may result in increased endothelial cell apoptosis, we established a procedure for the rapid isolation of liver endothelial cells and subsequent analysis by FACS. We isolated endothelial cells from the livers of 11- or 27-day-old mice that had been treated for 3 days with control IgG or mFlt(1-3)-IgG. This treatment schedule was not associated with neonatal mortality. We then determined the ratios of apoptotic endothelial cells by using an antibody directed against anti-CD31, which is expressed on the surface of endothelial cells (Vecchi et al., 1994), combined with annexin-V binding (Moore et al., 1998). As shown in Table 4, 18.9% of endothelial cells isolated from the liver of control animals were CD31 positive and 2.1% of these were positive for annexin-V. The ratio increased to 14.3% apoptotic, CD31-positive cells in mice treated with mFlt-IgG. At the same time, the level of CD31-positive endothelial cells dropped to 4.1% of the total cells isolated. Similar findings were obtained when we applied another, pan-endothelial cell marker, MECA 32 in the FACS analysis (data not shown). However, 27-day-old mice showed no significant changes in the numbers of CD31-positive cells nor in the ratios of annexin-V binding.

DISCUSSION

We adopted two independent approaches to inactive VEGF: conditional, Cre-*loxP*-mediated, VEGF– gene ablation, which achieves partial gene inactivation, and the administration of a soluble VEGF receptor chimeric protein, mFlt(1-3)-IgG, which results in a high degree of VEGF neutralization. Partial VEGF inactivation leads to impaired body growth and increased mortality. More profound inhibition results not only in nearly complete inhibition of somatic growth but also in abnormalities in a variety of organs, leading to rapidly lethal metabolic failure. Our findings indicate that VEGF-mediated

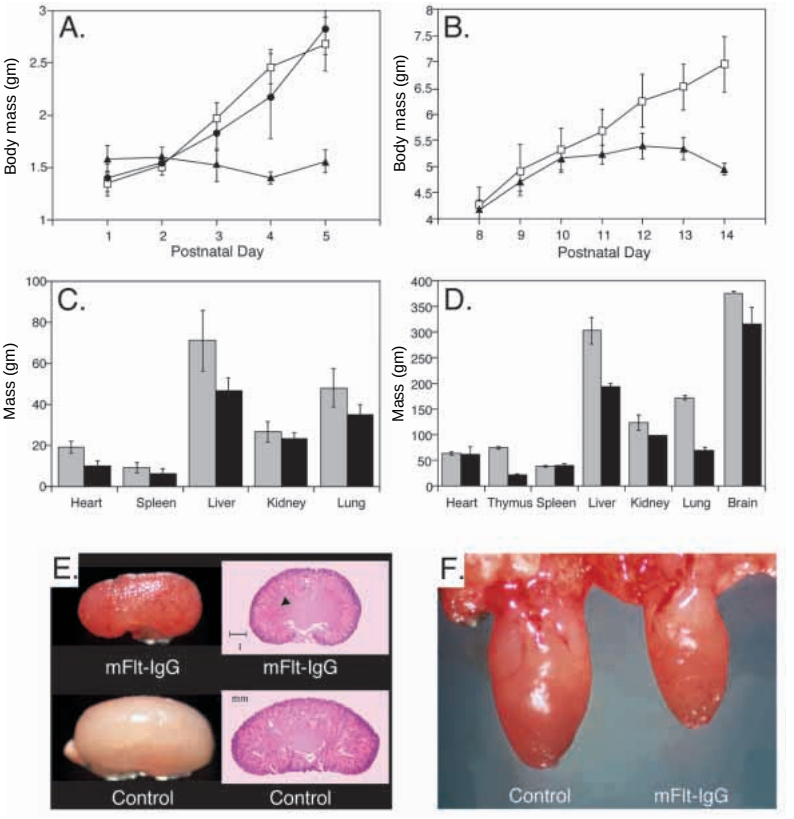

Fig. 4. Effect of mFlt(1-3)-IgG on body and organ mass. (A) Growth curve of mice treated with a control antibody (squares), PBS (circles) or mFlt(1-3)-IgG (triangles), starting at day 1 postnatally. Values are means ± s.d. (B) Growth curve of mice treated for 5 days with control IgG (n=10) (squares) or mFlt(1-3)-IgG (n=10) (triangles) starting at day 8. (C) Organ masses of 5-day-old mice, treated with control IgG (n=10), shown as tinted columns or mFlt(1-3)-IgG (n=10) for 4 days, shown in black. (D) Organ masses of 14-day-old mice treated for 5 days, starting at day 8, with control IgG (n=9), shown as tinted columns or mFlt-IgG (n=6), black columns. (E) Kidneys from 5-day-old neonate mice treated for 4 days. Kidneys from mFlt(1-3)-IgG-treated animals were smaller, had a granular surface appearance and showed punctuate areas of hemorrhage. The corresponding histological image shows interstitial hemorrhage at the corticomedullary junction (arrowhead). (F) Hearts from control and mFlt(1-3)-IgG-treated animals: hearts from mFlt(1-3)-IgG-treated animals were significantly smaller.

angiogenesis is a critical rate-limiting step in determining organ and body size. These findings are partially in contrast with a previous study, which examined the effects of an anti-VEGF polyclonal antiserum on newborn mice (Kitamoto et al., 1997). In agreement with our findings, the treatment resulted in inhibition of glomerular development. However, it did not affect body growth or survival nor did it induce lesions in organs other than kidney. This discrepancy probably reflects the lower inhibitory activity of the antiserum employed in that study relative to mFlt(1-3)-IgG.

Interestingly, the post-natal phenotype observed by us is unlike that observed following inactivation of a major growth regulatory molecule such as IGF-1. IGF-$1^{-/-}$ mice tend to die in utero, but those that survive after birth usually reach adulthood, in spite of a dramatically reduced body size (Baker et al., 1993). Therefore, impaired organ growth is not sufficient to account for the lethality observed in the present study and suggest additional mechanisms.

Although our studies do not directly address the actual kinetics of cell division and cell death, they suggest that a major reason for reduced body growth in VEGF*loxP*(+/+) and mFlt(1-3)-IgG-treated animals is reduced cell proliferation in all tissues analyzed. There was additional evidence of cell loss through increased levels of apoptosis of parenchymal cells within the heart, liver, pancreas and spinal ganglia of treated mice (Fig. 2C,G,H and data not shown), although the overall ratio did not exceed 1-3%. It should be noted that apoptosis (measured by TUNEL) is a more rapid process than the time taken to complete the S-phase of the cell cycle (measured by BrdU labeling). Therefore, we cannot rule out the possibility that slightly increased levels of apoptosis in the different tissues may represent a significant number when the numbers are compensated for the small time window of detection, as suggested by tumor inhibition studies (O'Reilly et al., 1997).

There is evidence that VEGF inhibits endothelial cell apoptosis in vitro (Gerber et al., 1998a,b) and it may function in vivo as a survival factor, at least for immature retinal vessels (Alon et al., 1995) and tumor vessels (Yuan et al., 1996). However, in contrast to parenchymal cells, we were unable to detect consistent differences in the levels of apoptotic endothelial cells in mFlt(1-3)-IgG-treated animals and in conditional knock out mice by applying the TUNEL staining technique (data not shown). This may be due, at least in part, to the fact that endothelial cells undergoing apoptosis tend to rapidly lose their attachment to the basement membrane (Augustin et al., 1995; Benjamin and Keshet, 1997). In addition, apoptotic endothelial cells may become the target of the immune system and thus are eliminated by phagocytes as soon as they manifest early signs of apoptosis. To overcome these limitations, we decided to employ a novel approach to assess endothelial cell apoptosis. We quantified apoptosis in endothelial cells freshly isolated from the liver of animals treated with mFlt(1-3)-IgG or control IgG. Such analysis revealed not only fewer endothelial cells overall but also a significant increase in the percentage of apoptotic endothelial cells, when the isolation was performed from mFlt(1-3)-IgG-treated neonates. Such findings demonstrate that endothelial cells undergo apoptotic cell death in response to VEGF inactivation. These findings are in

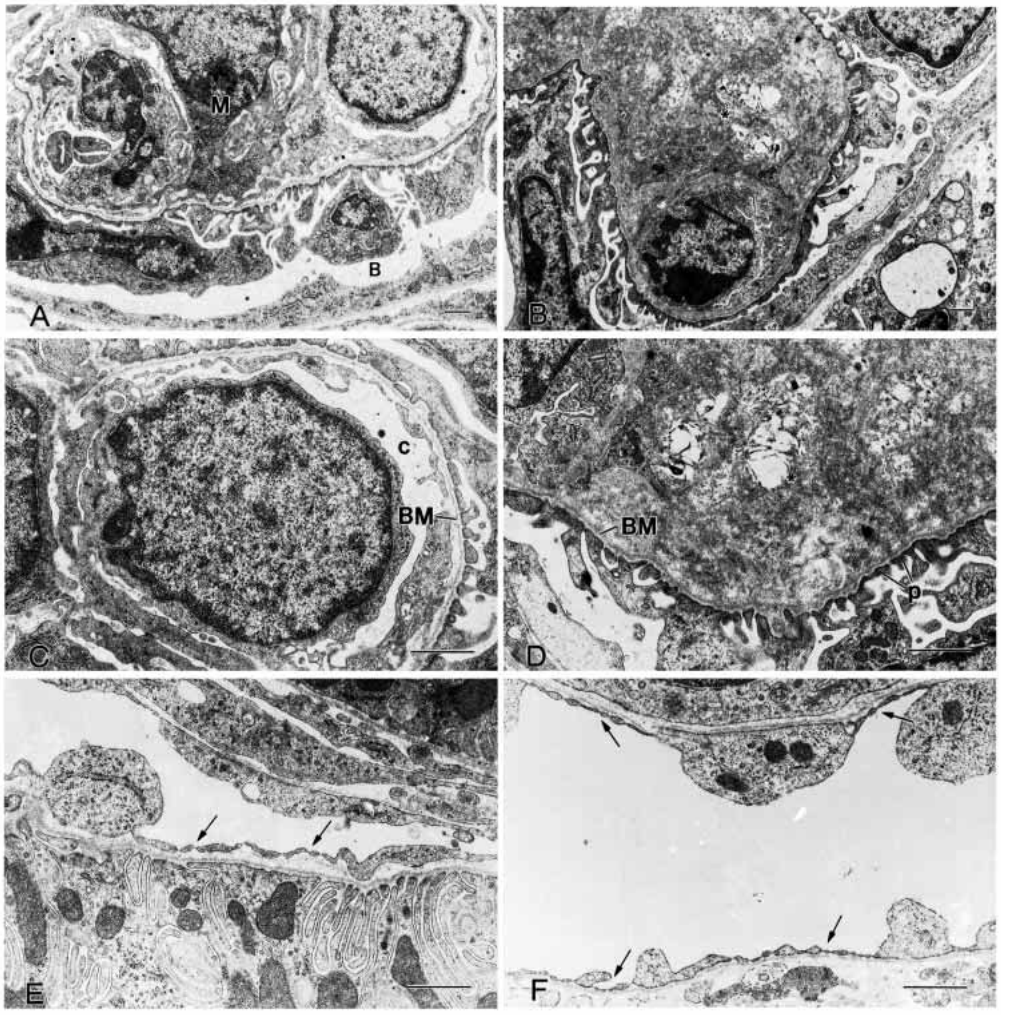

Fig. 5. Electron micrograph of glomeruli from control IgG (A,C,E) and mFlt(1-3)-IgG-treated (B,D,F) 4-day-old neonates. Severe mesangiolysis with loss of capillary architecture and disintegration of endothelial cells, accumulation of material (*), fibrils and thickening of the basement membrane (BM) can be seen in the mFlt(1-3)-IgG-treated animals. Processes of the podocytes (p) are in contact with the basement membrane. Arrows point to fenestrations in endothelial cells (E,F). Control kidneys displayed normal morphology (A,C,E). Bars, 1 μm.

agreement with the dramatic loss of Flk-1-positive cells and with the marked decrease in endothelial cells lining the vascular bed in liver and kidney, as assessed by ultrastructural analysis. Thus, apoptotic cell death may be a major contributor to the decrease in capillary vessels found in most organs after VEGF inactivation and eventually resulting in lethality.

VEGF has been associated with the development of fenestrations in endothelial cells (Roberts and Palade, 1995; Esser et al., 1998). In agreement with this hypothesis, we observed a reduction in the number of fenestrations in glomerular endothelial cells following mFlt(1-3)-IgG administrations. However, approximately half of the profiles examined demonstrated fenestrations, suggesting that factors other than VEGF are important in this process.

Considerable evidence indicates that VEGF plays a regulatory role in early hematopoiesis and implicates Flk-1/KDR in mediating such effects (Broxmeyer et al., 1995; Shalaby et al., 1995, 1997). Hematopoietic stem cells, megakaryocytes and platelets normally express this receptor (Katoh et al., 1995). Consistent with this hypothesis, we detected a decrease in platelet numbers following mFlt(1-3)-IgG administration. In contrast, the erythrocyte count did not fall below normal. This may be explained by a superimposed compensatory response to hypoxia, mediated by Epo (Jelkmann, 1992).

Although the emphasis of our study is on the role of VEGF in early postnatal development, it is important to stress that the dependence on VEGF is eventually lost when the animal matures and reaches adulthood. Treatment with mFlt-(1-3)-IgG failed to increase apoptosis in endothelial cells isolated from the liver of 27-day-old animals. Consistent with these findings, administration of mFlt(1-3)-IgG, starting at day 24, for up to 4 weeks, inhibited angiogenesis in areas of active proliferation but failed to induce mortality or any marked changes in blood chemistry, although it was associated with modest liver and glomerular changes (data not shown). A similar treatment failed to induce any significant histopathological abnormality in fully adult mice. Therefore, a process of maturation occurs, such that VEGF eventually is no longer essential for survival. This 'switch' seems to happen some time after the fourth postnatal week and, in the fully adult animal, VEGF may be required primarily for active angiogenic processes such as corpus luteum development or wound healing. The molecular and cellular nature of this switch remains elusive. Based on studies on the development of the retinal vasculature, it has been proposed that pericyte coverage may be the critical event that determines whether or not endothelial cells will be dependent on VEGF (Benjamin et al., 1998). However, our findings suggest that this is unlikely to be the only mechanism, since organ failure and lethality follow VEGF inactivation in the postnatal life, when the microvascular tree is already covered by pericytes (Hirschi and D'Amore, 1996).

Recently, several VEGF-related molecules have been identified, including PlGF, VEGF-B, VEGF-C and VEGF-D (Carmeliet and Collen, 1998; Enholm et al., 1998). It is known that PlGF and VEGF-B bind Flt-1 but not Flk-1/KDR In contrast, VEGF-C and VEGF-D bind the Flt-4 and Flk-1/KDR receptors. Therefore, it is possible that mFlt(1-3)-IgG may have interacted with PlGF or VEGF-B, raising the possibility that inactivation of these factors may contribute to the phenotype described in this study. However, considerable evidence indicates that binding to Flt-1 alone does not result in an effective mitogenic (Keyt et al., 1996) or antiapoptotic (Gerber et al., 1998b) signal in endothelial cells. Furthermore, inactivation of the PlGF gene in mice does not in result in any obvious abnormalities (Carmeliet and Collen, 1998).

In the present set of experiments, we chose a systemic approach to address the impact of VEGF inactivation in a whole body context and to assess the toxicity of anti-VEGF treatment in a rapidly growing organism. The availability of tissue-specific, conditional, knock out technology in mice may be instrumental in shedding light into the role of VEGF during development in specific organs, as well as in adult stages. This novel technique has the potential to locally delete the VEGF gene, while providing unimpaired levels of VEGF production in the rest of the body. For example, deletion of the VEGF gene

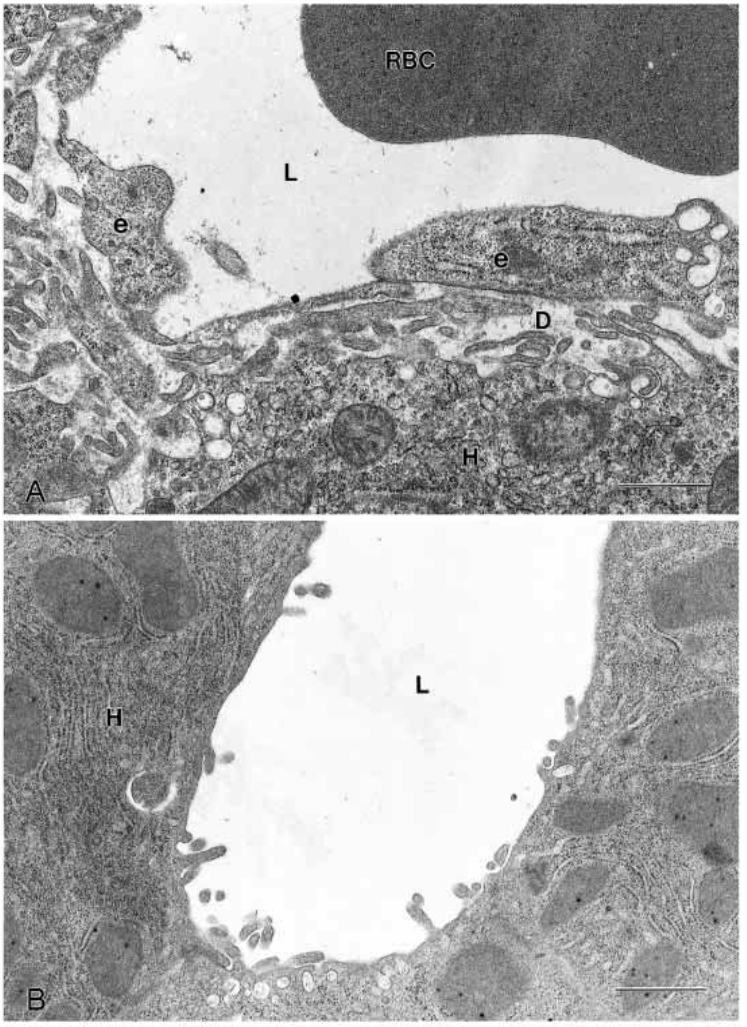

Fig. 6. Electron micrograph of the livers from control (A) and mFlt(1-3)-IgG treated (B) 4-day-old neonates. Note the absence of endothelial lining around a vascular lumen (L) in B. D, space of Disse; e, endothelial cells; H, hepatocytes. Bars, 1 μm.

in the embryonic heart or in the ventricles of adult mice may help in assessing the role of VEGF during heart development and may also be useful in the development of rational strategies for therapeutic intervention in ischemic heart disease.

We thank R. Latvala, J. Ross, H. Steinmetz and W. Wong for animal work, H. Prashad for cell culture, D. Peers for mFlt(1-3)-IgG purification, G. Meng and G. Hatami for assays, and D. Wood and L. Tamayo for graphics. We thank the Pathology laboratory and T.-N. Nguyen for in situ hybridization. We also thank S. Pitts-Meek, M. Bauer and M. Dowd for microinjections and M. Chu for genotype analysis. We are indebted to the oligonucleotide synthesis and DNA sequencing groups. We thank M. Gerritsen and D. Lowe for helpful discussions and advice.

REFERENCES

Alon, T., Hemo, I., Itin, A., Pe'er, J., Stone, J. and Keshet, E. (1995). Vascular endothelial growth factor acts as a survival factor for newly formed retinal vessels and has implications for retinopathy of prematurity. *Nat. Med.* **1,** 1024-028.

Augustin, H. G., Braun, K., Telemenakis, I., Modlich, U. and Kuhn, W. (1995). Ovarian angiogenesis. Phenotypic characterization of endothelial cells in a physiological model of blood vessel growth and regression. *Am. J. Pathol.* **147,** 339-351.

Baker, J., Liu, J. P., Robertson, E. J. and Efstratiadis, A. (1993). Role of insulin-like growth factors in embryonic and postnatal growth. *Cell* **75,** 73-82.

Benjamin, L., Hemo, I. and Keshet, E. (1998). A plasticity window for blood vessel remodelling is defined by pericyte coverage of the preformed endothelial network and is regulated by PDGF-B and VEGF. *Development* **125,** 1591-1598.

Benjamin, L. E. and Keshet, E. (1997). Conditional switching of vascular endothelial growth factor (VEGF) expression in tumors: induction of endothelial cell shedding and regression of hemangioblastoma-like vessels by VEGF withdrawal *Proc. Natl. Acad. Sci. USA* **94,** 8761-8766.

Borgström, P., Bourdon, M. A., Hillan, K. J., Sriramarao, P. and Ferrara, N. (1998). Neutralizing anti-vascular endothelial growth factor antibody completely inhibits angiogenesis and growth of human prostate carcinoma micro tumors in vivo. *Prostate* **35,** 1-10.

Brooks, P. C., Montgomery, A. M., Rosenfeld, M., Reisfeld, R. A., Hu, T., Klier, G. and Cheresh, D. A. (1994). Integrin alpha v beta 3 antagonists promote tumor regression by inducing apoptosis of angiogenic blood vessels. *Cell* **79,** 1157-1164.

Broxmwyer, H. E., Cooper, S., Li, Z. H., Song, H. Y., Kwon, B. S., Warren, R. E., Donner, D. B. (1995). Myeloid progenitor cell regulatory effects of vascular endothelial growth factor. *Int. J. Hematol*. **62**, 203-215.

Carmeliet, P. and Collen, D. (1998). Vascular development and disorders: Molecular analysis and pathogenic insights. *Kidney Internat.* **53,** 1519-1549.

Carmeliet, P., Ferreira, V., Breier, G., Pollefeyt, S., Kieckens, L., Gertsenstein, M., Fahrig, M., Vandenhoeck, A., Harpal, K., Eberhardt, C., Declercq, C., Pawling, J., Moons, L., Collen, D., Risau, W. and Nagy, A. (1996). Abnormal blood vessel development and lethality in embryos lacking a single VEGF allele. *Nature* **380,** 435-439.

Clapp, C., Martial, J. A., Guzman, R. C., Rentier-Delrue, F. and Weiner, R. I. (1993). The 16-kilodalton N-terminal fragment of human prolactin is a potent inhibitor of angiogenesis. *Endocrinology* **133,** 1292-1299.

Davis-Smyth, T., Chen, H., Park, J., Presta, L. G. and Ferrara, N. (1996). The second immunoglobulin-like domain of the VEGF tyrosine kinase receptor Flt-1 determines ligand binding and may initiate a signal transduction cascade. *EMBO J.* **15**, 4919-4927.

Enholm, B., Jussila, L., Karkkainen, M. and Alitalo, K. (1998).Vascular endothelial growth factor-C: A growth factor for lymphatic and blood vessel endothelial cells. *Trends Cardiovasc. Med.* **8**, 292-296

Esser, S., Wolburg, K., Wolburg, H., Breier, G., Kurzchalia, T. and Risau, W. (1998). Vascular endothelial growth factor induces endothelial fenestrations in vitro. *J. Cell Biol.* **140,** 947-959.

Ferrara, N., Carver Moore, K., Chen, H., Dowd, M., Lu, L., O'Shea, K. S., Powell Braxton, L., Hillan, K. J. and Moore, M. W. (1996). Heterozygous embryonic lethality induced by targeted inactivation of the VEGF gene. *Nature* **380,** 439-442.

Ferrara, N., Chen, H., Davis-Smyth, T., Gerber, H.-P., Nguyen, T.-N., Peers, D., Chisholm, V., Hillan, K. J. and Schwall, R. H. (1998). Vascular endothelial growth factor is essential for corpus luteum angiogenesis. *Nat. Med.* **4,** 336-340.

Ferrara, N. and Davis-Smyth, T. (1997). The biology of vascular endothelial growth factor. *Endocr. Rev.* **18,** 4-25.

Fong, G. H., Rossant, J., Gertsenstein, M. and Breitman, M. L. (1995). Role of the Flt-1 receptor tyrosine kinase in regulating the assembly of vascular endothelium. *Nature* **376,** 66-70.

Gerber, H. P., Dixit, V. and Ferrara, N. (1998a). Vascular endothelial growth factor induces expression of the antiapoptotic proteins Bcl-2 and A1 in vascular endothelial cells. *J. Biol. Chem.* **273,** 13313-13316.

Gerber, H. P., McMurtrey, A., Kowalski, J., Yan, M., Keyt, B., Dixit, V. and Ferrara, N. (1998b). VEGF regulates endothelial cell survival by the PI3-kinase/Akt Signal transduction pathway. Requirement for Flk-1/KDR activation. *J. Biol. Chem.* **273,** 30336- 30345.

Gibson, U. E. M., Heid, C. A. and Williams, P. M. (1996). A novel method for real time quantitative RT-PCR. *Genome Res.* **6**, 995-1001

Good, D., Polverini, P., Rastinejad, F., Beau, M., Lemons, R., Frazier, W. and Bouck, N. (1990). A tumor suppressor-dependent inhibitor of angiogenesis is immunologically and functionally indistinguishable from a fragment of thrombospondin. *Proc. Natl. Acad. Sci. USA* **87,** 6624-6628.

Gu, H., Marth, J. D., Orban, P. C., Mossmann, H. and Rajewsky, K. (1994). Deletion of a DNA polymerase beta gene segment in T cells using cell type-specific gene targeting. *Science* **265,** 103-106.

Hamilton, W. J, Boyd, J. D. and Mossman, H. W. (1962). *Human Embryology*. William & Wilkins, Baltimore.

Heid, C. A., Stevens, J., Livak, K. J. and Williams, P. M. (1996). Real time quantitative PCR. *Genome Res.* **6,** 986-994.

Hiratsuka, S., Minowa, O., Kuno, J., Noda, T. and Shibuya, M. (1998). Flt-1 lacking the tyrosine kinase domain is sufficient for normal development and angiogenesis in mice. *Proc. Natl. Acad. Sci. USA* **95,** 9349-9354.

Hirschi, K. K. and D'Amore, P. A. (1996). Pericytes in the microvasculature. *Cardiovasc. Res.* **32,** 687-698.

Hogan, B., Beddington, R., Costantini, F. and Lacy, E. (1994). *Manipulating the Mouse Embryo*, 2nd edition. New York: Cold Spring Harbor Laboratory Press.

Huang, S., Hendriks, W., Althage, A., Hemmi, S., Bluethmann, H., Kamijo, R., Vilcek, J., Zinkernagel, R. M. and Aguet, M. (1993). Immune response in mice that lack the interferon-gamma receptor. *Science* **259**, 1742-1745.

Jelkmann, W. (1992). Erythropoietin: structure, control of production and function. *Physiol. Rev.* **72,** 449-489.

Katoh, O., Tauchi, H., Kawaishi, K., Kimura, A. and Sarow, Y. (1995). Expression of the vascular endothelial growth factor (VEGF) receptor gene, KDR, in hematopietic cells and inhibitory effects of VEGF on apoptotic cell death caused by ionizing radiations. *Cancer Res.* **55**, 5687-5692.

Keyt, B. A., Nguyen, H. V., Berleau, L. T., Duarte, C. M., Park, J., Chen, H. and Ferrara, N. (1996). Identification of vascular endothelial growth factor determinants for binding KDR and FLT-1 receptors. Generation of receptor-selective VEGF variants by site-directed mutagenesis. *J. Biol. Chem.* **271,** 5638-5646.

Kitamoto, Y., Tokunaga, H. and Tomita, K. (1997). Vascular endothelial growth factor is an essential molecule for mouse kidney development. *J. Clin. Invest.* **99,** 2351-2357.

Kuhn, R., Schwenk, F., Aguet, M. and Rajewsky, K. (1995). Inducible gene targeting in mice. *Science* **269,** 1427-1429.

Monacci, W. T., Merrill, M. J. and Oldfield, E. H. (1993). Expression of vascular permeability factor/vascular endothelial growth factor in normal rat tissues. *Am. J. Physiol.* **264,** C995-1002.

Moore, A., Donahue, C., Bauer, K. D. and Mather, J. P. (1998). Simultaneous measurement of cell cycle and apoptotic cell death. In *Methods in Cell Biology* (ed. J. P. Mather)), pp. 266 -278. Academic Press.

Nehls, V. and Drenckhahn, D. (1993). The versatility of microvascular pericytes: From mesenchyme to smooth muscle? *Histochemistry* **99,** 1-12.

O'Reilly, M. O., Boehm, T., Shing, Y., Fukai, N., Vasios, G., Lane, W. S., Flynn, E., Birkhead, J. R., Olsen, B. R. and Folkman, J. (1997). Endostatin: An endogenous inhibitor of angiogenesis and tumor growth. *Cell* **88,** 277-285.

O'Reilly, M. S., Holmgren, L., Shing, Y., Chen, C., Rosenthal, R. A., Moses, M., Lane, W. S., Cao, Y., Sage, E. H. and Folkman, J. (1994). Angiostatin: a novel angiogenesis inhibitor that mediates the suppression of metastases by a Lewis lung carcinoma. *Cell* **79,** 315-328.

Patan, S., Haenni, B. and Burri, P. H. (1997). Implementation of intussusceptive microvascular growth in the chicken chorioallantoic membrane (CAM). *Microvasc. Res.* **53,** 33-52.

Presta, L. G., Chen, H., O'Connor, S. J., Chisholm, V., Meng, Y. G., Krummen, L., Winkler, M. and Ferrara, N. (1997). Humanization of an anti-VEGF monoclonal antibody for the therapy of solid tumors and other disorders. *Cancer Res.* **57,** 4593-4599.

Quinn, T. P., Peters, K. G., De Vries, C., Ferrara, N. and Williams, L. T. (1993). Fetal liver kinase 1 is a receptor for vascular endothelial growth factor and is selectively expressed in vascular endothelium. *Proc. Natl. Acad. Sci. USA* **90,** 7533-7637.

Ribelin, W. E. and Cox, J. R. (1965). *The Pathology of Laboratory Animals.* Springfield: Charles C. Thomas.

Risau, W. (1995). Differentiation of endothelium. *FASEB J.* **9,** 926-933.

Risau, W. (1997). Mechanisms of angiogenesis. *Nature* **386,** 671-674.

Roberts, W. G. and Palade, G. E. (1995). Increased microvascular permeability and endothelial fenestration induced by vascular endothelial growth factor. *J. Cell Sci.* **108,** 2369-2379.

Sage, E. H., Bassuk, J. A., Vost, J. C., Folkman, M. J. and Lane, T. F. (1995). Inhibition of endothelial cell proliferation by SPARC is mediated through a Ca (2+)-binding EF-hand sequence. *J. Cell Biochem.* **57,** 127-140.

Shalaby, F., Rossant, J., Yamaguchi, T. P., Gertsenstein, M., Wu, X. F., Breitman, M. L. and Schuh, A. C. (1995). Failure of blood-island formation and vasculogenesis in Flk-1-deficient mice. *Nature* **376,** 62-66.

Shalaby, F., Ho, J., Stanford, W. L., Fisher, K. D., Schuh, A. C., Schwartz, L., Bernstein, A. and Rossant, J. (1997). A requirement for flk-1 in primitive and definitive hematopoiesis. *Cell* **89**, 981-990.

Vecchi, A., Garlanda, C., Lampugnani, M. G., Resnati, C., Matteucci, C., Stoppacciaro, A., Schnurch, H., Risau, W., Ruco, L., Mantovani, A. and Dejana, E. (1994). Monoclonal antibodies specific for endothelial cells of mouse blood vessels. Their application in the identification of adult and embryonic endothelium. *Eur. J. Cell Biol.* **63,** 247-254.

West, J. B. (1990). *Physiological Basis of Medical Practice*. Baltimore: William and Wilkins.

Yuan, F., Chen, Y., Dellian, M., Safabakhsh, N., Ferrara, N. and Jain, R. K. (1996). Time-dependent vascular regression and permeability changes in established human tumor xenografts induced by an anti-vascular endothelial growth factor/vascular permeability factor antibody. *Proc. Natl. Acad. Sci. USA* **93,** 14765-14770.